ENGINEERING RESEARCH JOURNAL (ERJ)

Vol. 1, No. 39 January 2019, pp. 86-93.

Journal Homepage: www.feng.bu.edu.eg

Experimental study on convective heat transfer and pressure drop of water flow inside conically coiled tube-in-tube heat exchanger

M.A. Radwan(1,*), M.R. Salem(2), H.A. Refaey(2) and M.A. Moawed(2)

(1)Operation Department at Benha Power Station Plant, Benha, Egypt.

(2)Department of Mechanical Engineering, Faculty of Engineering at Shoubra, Benha University, 11629 Cairo, Egypt.

Abstract

The present work is devoted to experimentally investigate the characteristics of the convective heat transfer and pressure drop of pure water in the tube side of vertical helically/conically coiled tube in tube heat exchangers. This work is performed at different geometrical parameters of the coils and at different operating conditions of the tube side. Six concentric coiled tube in tube heat exchangers of counter-flow configurations are constructed; three are helically coiled with different torsions, and the others are conically coiled with taper angle of 45º. Wilson plot method is used to investigate the thermal performance results in terms of tube average heat transfer coefficient, average Nusselt number and fanning friction factor. The results showed that the internal tube of conical heat exchangers has a lower heat transfer coefficient and lower friction factor compared with that in the helical coil, while the conical coil of taper angle 45° provides a higher hydrothermal performance compared with the helical coil. Empirical correlations are developed to predict the tube-average Nusselt number and fanning friction factor.

Keywords: Helical and conical coils; Heat exchanger; Nusselt number; Friction.

Introduction

Heat exchangers are used extensively in variety of applications, like chemical processing, nuclear reactors, power plants, heat recovery systems, food industries and in refrigeration and air-conditioning systems. The enhancement in heat transfer coefficient has two important outcomes in the heat exchangers. Firstly, it improves the performance and secondly it reduces the size of the heat exchanger. In applications, many techniques are used to enhance the heat transfer and are classified in two types as active and passive techniques. Coiled tube configuration in the heat exchangers is the one of the important passive heat transfer enhancement techniques [1, 2], due to high heat transfer coefficient and compact structure.

Helical coiled configuration is very effective for some heat transfer equipment such as heat exchangers [3, 4] and reactors due to the relatively large heat transfer area with relative to the small space (volume) occupied. The curvature of the coiled tube induces secondary flow patterns [5] due to the centrifugal force, which allow good mixing for the fluid layers and consequently enhances the heat transfer coefficient, whereas pressure drop across the coiled tube increases. It was noted by Shah and Joshi [6], that the enhancement depends on the intensity of secondary developed in the coiled tube. In case of smaller coil diameter and tube diameters, the intensity of secondary flow developed was high. Eustice [7] presented the first observation for the fluid motion in curved pipes. Then, many researchers [2, 8] followed this work, where they provided the flow and temperature fields analyses experimentally and numerically. Prabhanjan et al. [4] performed a comparative study of the heat transfer between straight and helically coiled tubes. They showed that the coiled tube heat exchangers provided a higher heat transfer coefficient. Thermal performance characteristics of a helical heat exchanger was investigated by San et al. [9]. The helical coil heat exchanger considered for the analysis was rectangular cross section and cover plates. The analysis of water-water heat exchanger was numerically carried out by Seara et al. [10]. The analysis was validated with experimental data with two helically coiled tube heat exchangers tested under the same operating conditions. The analysis illustrated that the Nusselt number was augmented with increasing in tube diameter. Lee et al. [11] also studied the effect of buoyancy forces on fully developed laminar flow on the flow and thermal fields. They found that the rotation of the secondary flow patterns depended on the buoyancy forces.

This was also confirmed by Padmanabhan [12] who indicated that he secondary motion was affected by buoyancy forces.

An investigation on helically coiled tube in tube heat exchangers was experimentally performed by Gomaa et al. [13]. The coil curvature ratio, number of turns, flow configuration were the considered parameters for the study. The results showed that the annulus Nusselt number and friction factor were affected by the annulus curvature ratio and number of turns. Mandal and Nigam [14] studied the transfer and fluid flow under turbulent conditions. Salem et al. [15-17] conducted a series of experimental investigations on a horizontal shell and coil heat exchanger. They investigated the effect of the coil curvature and torsion in addition to the effect of using nanofluid in the internal tube at different operating conditions for both sides of the heat exchanger. They developed correlations to predict the average Nusselt number in the tube and shell side in addition to the Fanning friction factor in the tube side. The present work is devoted to experimentally compare thermal performance characteristics of vertical helically and conically coiled tube in tube heat exchangers of counter-flow configurations. This work is performed at different geometrical parameters of the coils turions (pitch ratios) and different operating conditions for the tube side of the heat exchanger.

2. Experimental apparatus

The apparatus used in this study comprises hot and cold loops. The hot circuit consists of heating unit, pump, valves, flow meter, internal plain tube and the connecting pipes. The cold circuit consists of a cooling unit, pump, valves, flow meter, annular pipe and the connecting pipes. Fig. 1 is a schematic diagram of the experimental setup. Two variable area flow meters; 1.8–18 l/min flow rate range, are used to measure the volume flow rates of the two main loops fluids. Four K-type thermocouples (wires of 0.2 mm diameter) are directly inserted into the flow streams, at approximately 60 mm from the heat exchanger ports, to measure the inlet and exit temperatures of the annulus and tube fluids. A digital differential pressure transducer is employed for measuring the pressure drop of water between the tube inlet and outlet with an accuracy of ±1% of full scale. Six coiled tube-in-tube heat exchangers (Fig. 2) are constructed and fabricated with the characteristic dimensions represented in Table 1.

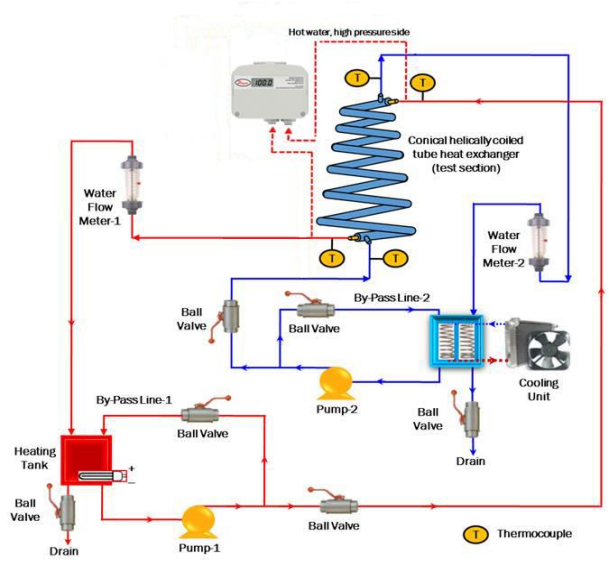

Fig. 1: Schematic diagram of the experimental setup.

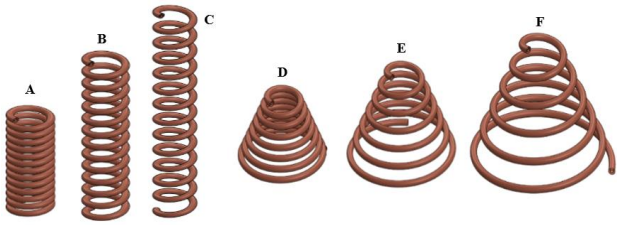

Fig. 2: Schematic diagram of the coils.

Table 1: Characteristic dimensions of the used coils.

Coil	$d_{t,i}$ (mm)	$d_{t,o}$ (mm)	$d_{an,i}$ (mm)	L_t (mm)	$D_{c,min}$ (mm)	S (mm)	θ	λ	N
A	8.3	9.52	17.65	5000	119.05	10	0°	0.0777	15.92
B						20		0.1044	
C						30		0.1311	
D						Variable	45°	0.0777	6.47
E								0.1044	5.57
F								0.1311	4.96

3.1 Experimental Procedure

Firstly, the thermocouples are attached at the inlet and outlet of the annulus and internal tube sides. Then, the following parts are assembled to initiate the experiments: the heat exchanger, heating and cooling units, pumps, piping, flow meters, thermocouples and the differential pressure transducer. The first step to collect the data from the system is to fill the heating and the cooling tanks with water from the domestic water supply. Then, the heater, the cooling unit and the pumps are turned on. The inlet temperatures of the fluids in both sides are adjusted by regulating the temperatures of the heating and cooling tanks through their thermostats. The flow rates are adjusted through the flow meters and the installed valves, which are regulated to obtain the required flow rates in the primary lines and the remainder is bypassed to the reservoirs. The range of the operating conditions is given in Table 2. During the test operation, the steady-state condition is conducted when a maximum variation of

0.5℃ for each thermocouple reading within 20 minutes is recorded.

Table 2: Range of operating conditions.

Parameters/operating conditions	Range or Value
Tube-side	
Water flow rate, l/min	6.01–18.26 ($21207 \leq Re_t \leq 91054$)
Inlet temperature, °C	40, 50, 60 ($3.25 \leq Pr_t \leq 4.83$)
Annulus-side	
Water flow rate, l/min	8.06
Inlet temperature, °C	20

4. Data Reduction

Microsoft Excel sheets are prepared to process the experimental data for the heat transfer coefficients and pressure drop. It should be noted that for all calculations, the properties of the fluids of the annulus and tube-sides are calculated at the bulk temperatures, $T_{an,m}$ and $T_{t,m}$, respectively. The water thermophysical properties are evaluated from Remsburg [18].

$$T_{an,m} = \frac{T_{an,i} + T_{an,o}}{2} \quad (1)$$

$$T_{t,m} = \frac{T_{t,i} + T_{t,o}}{2} \quad (2)$$

The primary measurements in heat transfer calculations consist of six variables, namely the flow rates and the inlet and outlet temperatures of both streams of the heat exchanger. The heat transfer rates on the internal tube and annulus sides (Q_t and Q_{an}) are calculated by;

$$Q_t = \dot{m}_t Cp_t (T_{t,i} - T_{t,o}) \quad (3)$$

$$Q_{an} = \dot{m}_{an} Cp_{an} (T_{an,o} - T_{an,i}) \quad (4)$$

Assuming that the measurements are sufficiently accurate without heat gain or loss, there is an energy balance between the two streams ($Q_t = Q_{an}$). While in the real experiments, there would always be some discrepancy between the two rates. Therefore, the arithmetical mean of the two, Q_{ave}, can be used as the heat load of the exchanger. For all experimental tests, the heating and cooling loads calculated from the hot and cold sides do not differ by more than $\pm 3.9\%$.

$$Q_{ave} = \frac{|Q_t| + |Q_{an}|}{2} \quad (5)$$

The overall thermal conductance is calculated from this heat load, the temperature data and flow rates using Eq. (6);

$$U_i A_{t,i} = \frac{Q_{ave}}{\Delta T_{L.M}} \quad (6)$$

Neglecting the thermal resistances of the tube wall and fouling, the overall thermal conductance can be expressed in terms of the thermal resistances.

$$\frac{1}{U_i A_{t,i}} = \frac{1}{\bar{h}_{an} A_{t,o}} + \frac{1}{\bar{h}_t A_{t,i}} \quad (7)$$

The average Nusselt number ($\overline{Nu}_t$) for the tube-side fluid, can be obtained as follows;

$$\overline{Nu}_t = \frac{\bar{h}_t \, d_{t,h}}{k_t} \quad (8)$$

Tube Reynolds number can be written as follows;

$$Re_t = \frac{4\dot{m}_t}{\pi d_{t,i} \mu_t} \quad (9)$$

The tube-side Stanton number (St_t) is determined as follows;

$$St_t = \frac{\overline{Nu}_t}{Re_t . Pr_t} \quad (10)$$

In the present study, the measurement of the friction factor in the annulus-side is conducted at the same time as the heat transfer measurements. The fanning friction factor for the fluid in circulation inside the tube side (f_t) is calculated with the following equation;

$$f_t = \frac{\Delta P_t \, d_{t,h}}{2 L_t \rho_t u_t^2} \quad (11)$$

$$u_t = \frac{\dot{V}_t}{\frac{\pi}{4} d_{t,i}^2} \quad (12)$$

5. Apparatus Validation and Data Verification

Using the aforementioned experimental procedures and analysis methods, the validation of the methodologies in determining the annulus heat transfer coefficient and friction factor is performed by taking measurements for the flow in the tube side and comparing it with established heat transfer and friction factor correlations. For heat transfer calculations, the experimental procedures are validated by comparing the results of $\overline{Nu}_t$ for the water flowing through the internal tube with $\overline{Nu}_t$ for turbulent flow developed by [19] and [17]. For the Fanning friction factor in in the internal tube, the procedures are validated by comparing the results of f_t for the water flowing through the internal tube with f_t for turbulent flow developed by [20] and [17]. The results of these comparisons are shown in Fig. 4. The range of the operating conditions during validation is given in Table 3.

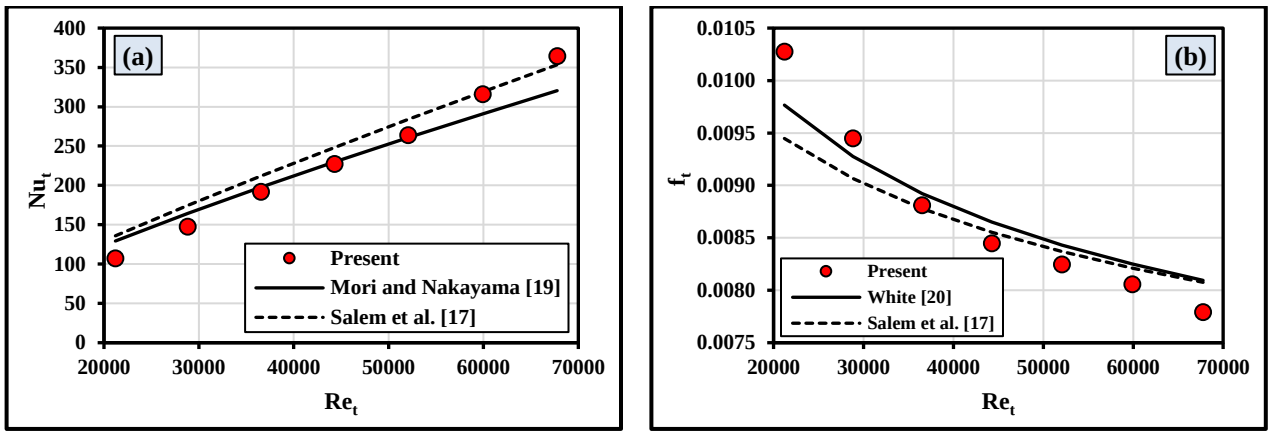

Fig. 3: Validation of the experimental data (a) average Nusselt number (b) Fanning friction factor.

It is clear that the experimental results for both heat transfer and friction factor calculations are in good agreement with previous studies, with maximum value of the average deviation of ±9.3% and ±3.1% for $\overline{Nu}_t$ and f_t.

6. Results and Discussion

6.1 Effect of Coil Taper Angle

Figure 4 represents a sample of the results or varying the coil taper angle from 0° to 45° at $\lambda = 0.1044$ and $T_{ti} = 50°C$.

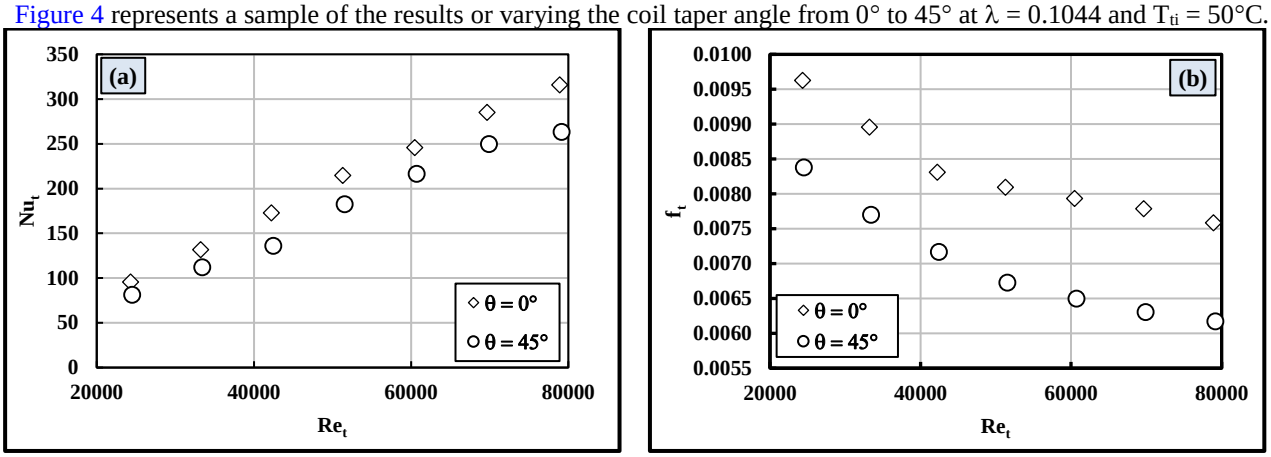

Fig. 4: Variation of the tube (a) average Nusselt Number and (b) friction factor with tube Reynolds number at different coil taper angles.

It is indicated that increasing the coil taper angle from 0° to 45° reduces both the tube average Nusselt number and friction factor by 15.6% and 15.8%, respectively. This can be attributed to the decrease in the coil curvature ratio (the coil mean diameter increases) and consequently the centrifugal forces and the induced secondary flow are decreased.

6.2 Effect of Coil Torsion

Figure 5 illustrates a sample of the results for varying the coil torsion from 0.0777 to 0.1311 at $\theta = 0°$, $T_{ti} = 60°C$.

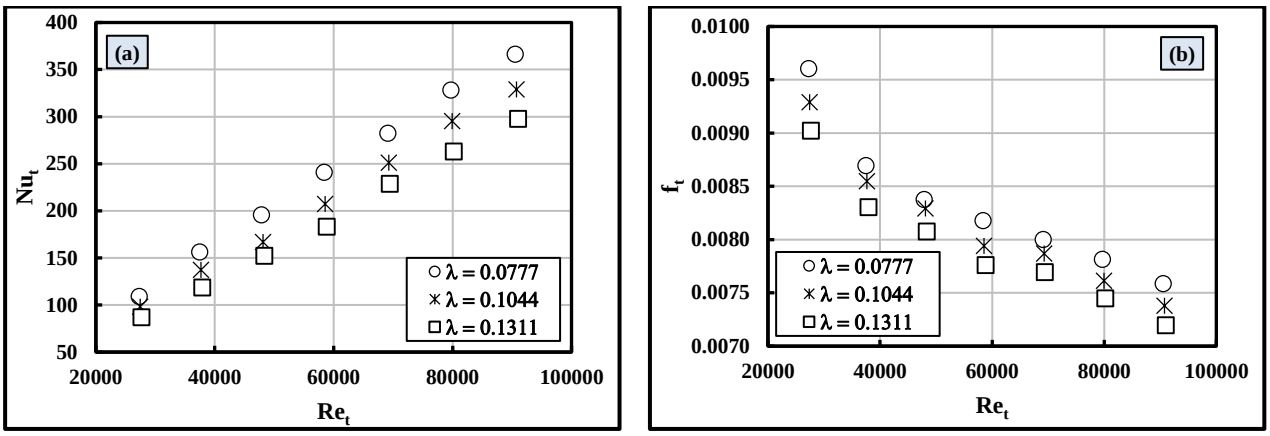

Fig. 5: Variation of the tube (a) average Nusselt Number and (b) friction factor with tube Reynolds number at different coil torsions.

It is evident that increasing the coil torsion 0.0777 to 0.1311 reduces both the tube average Nusselt number and friction factor by 22.1% and 5.3%, respectively. This can be attributed to the increase in rotational force as a result of increasing the coil torsion, which diminishes the secondary flow formation that established by the centrifugal effect.

6.3 Influence of Tube Operating Conditions

Figure 6 illustrates a sample of the results for varying the tube side water inlet temperature from 40°C to 60°C at coil taper angle 0° and λ = 0.0777 for the range of tube side Reynolds number from 21208 to 91054.

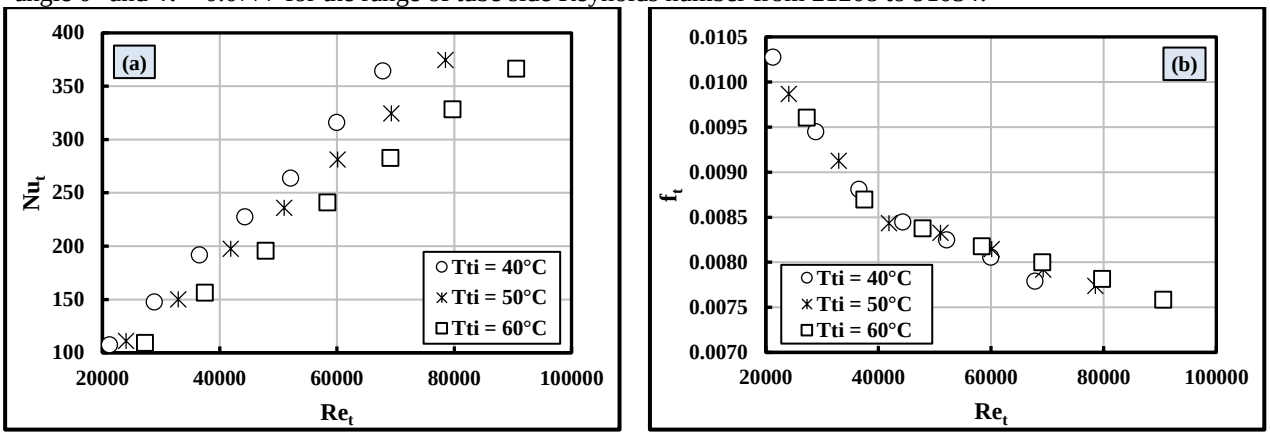

Fig. 6: Variation of the tube (a) average Nusselt Number and (b) friction factor with tube Reynolds number at different tube side inlet temperature.

It is obvious that increasing the tube-side water inlet temperature from 40°C to 60°C reduces the tube average Nusselt number. This can be attributed to the decrease in fluid Prandtl number with increasing its temperature. Besides, it is shown that there is nearly no effect on the flow friction factor by varying the water inlet temperature. This is due the tiny change in the water viscosity with changing its temperature. Additionally, it is clear t that the tube side average Nusselt number increases with increasing water Reynolds number. This due to increasing the flow turbulence level in addition to increasing the centrifugal force effect, which induces more effective secondary flow. While the flow friction factor decreases with increasing water Reynolds number. This is due to increasing the momentum force relative to the viscous force.

7. Hydrothermal Performance Index

The combined hydrothermal performance index (HTPI) is determined using St_t and f_t ratios [21] that are calculated using the values obtained for taper angle 45° and 0°, as follows;

$$HTPI = \frac{St_{45°}/St_{0°}}{\left(f_{t,45°}/f_{t,0°}\right)^{1/3}} \quad \textbf{(13)}$$

The average HTPI is calculated and the results are illustrated in Fig. 7 for different coil torsions.

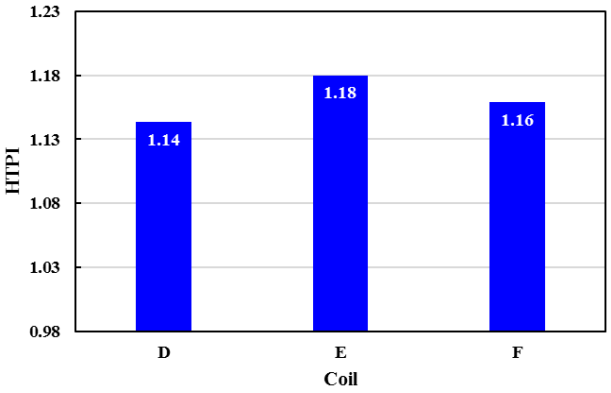

Fig. 7: The hydrothermal performance index.

It is obvious that the *HTPI* is more than unity for all ranges of investigated parameters. Also, it is noticeable that the coil of pitch ratio of 0.1044 provides the highest *HTPI*.

8. Correlations

Using the present experimental data, correlations are developed to predict the tube-average Nusselt number and fanning friction factor. The tube-average Nusselt number is correlated as a function of its Reynolds and Prandtl numbers, and coil taper angle and pitch ratios as follows;

$$\overline{Nu}_t = 0.000157\, Re_t^{1.083}\, Pr_t^{0.735} \left(\frac{1+\theta}{180}\right)^{-0.044} \lambda^{-0.489} \quad (14)$$

Additionally, a correlation for tube-side fanning friction factor is obtained as follows;

$$f_t = 0.0645\, Re_t^{-0.2329} \left(\frac{1+\theta}{180}\right)^{-0.0454} \lambda^{-0.0975} \quad (15)$$

Eqs. (14) and (15) are valid for $21208 \le Re_t \le 91054$, $3.25 \le Pr_t \le 4.83$, $0 \le \theta \le 45°$, and $0.0777 \le \lambda \le 0.1311$. Comparisons of the experimental $\overline{Nu}_t$ and f_t with those predicted by the proposed correlations are illustrated in Fig. 8.

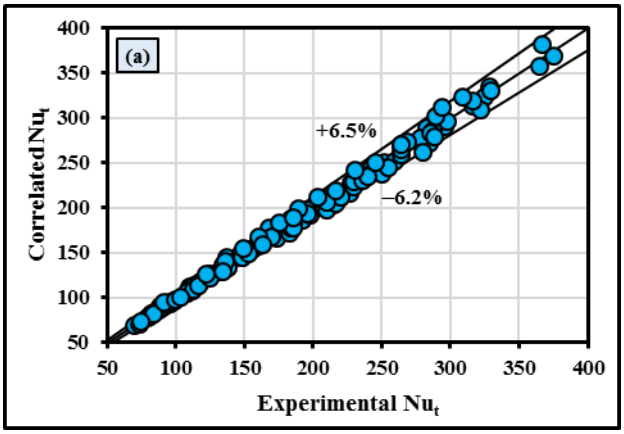

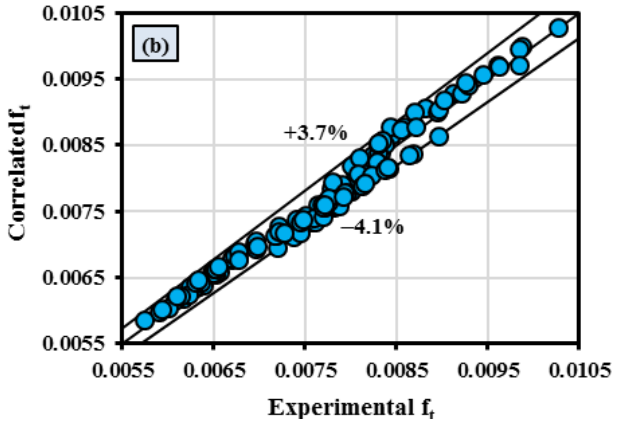

Fig. 8: Comparisons of the present experimental values with that correlated by; (a) Eq. (14), (b) Eq. (15).

From this figure, it is obvious that the proposed correlations are in good agreement with the present experimental data. It is evidently seen that the data falls of the proposed equations within maximum deviations of $\pm 6.5\%$ and $\pm 4.1\%$ for $\overline{Nu}_{an}$ and f_{an}, respectively.

9. Conclusions

From the previous sections and according to the results obtained using the experimental investigation, the following conclusions can be expressed:

- The internal tube of conical heat exchangers has a lower heat transfer coefficient and lower friction factor compared with that in the helical coil.
- The heat transfer coefficient and friction factor in the internal tube increase with decreasing cone angle, coil torsion and water inlet temperature and with increasing the flow Reynolds number.
- The effect of the tube-fluid inlet temperature on its friction factor can be neglected.
- The conical coil of taper angle 45° provides a higher hydrothermal performance compared with the helical coil.
- The conical coil of taper angle 45° and torsion of 0.1044 provides the highest hydrothermal performance index.
- Empirical correlations are developed to predict the tube-average Nusselt number and fanning friction factor.

References

[1] N. Acharya, M. Sen, H.C. Chang, "Thermal entrance length and Nusselt numbers in coiled tubes", International Journal of Heat and Mass Transfer, Vol. 37(2), pp. 36-340, 1993.

[2] N. Acharya, M. Sen, H.C. Chang, "Analysis of heat transfer enhancement in coiled-tube heat exchangers", International Journal of Heat and Mass Transfer, Vol. 44, pp. 3189-3199, 2001.

[3] L.A.M.Janssen, C.J. Hoogendoorn, "Laminar convective heat transfer in helical coiled

tubes", International Journal of Heat and Mass Transfer, Vol. 21, pp. 1197-1206, 1978.

[4] D.G. Prabhanjan, G.S.V. Raghavan, T.J. Rennie, "Comparison of heat transfer rates between a straight tube heat exchanger and a helically coiled heat exchanger", International Communication in Heat Mass Transfer, Vol. 29(2), pp 185–191, 2002.

[5] A.N. Dravid, K.A. Smith, E.W. Merrill, P.L.T. Brian, "Effect of secondary fluid motion on laminar flow heat transfer in helically coiled tubes", AIChE Journal, Vol. 17(5), pp. 1114-1122, 1971.

[6] R.K. Shah, S.D. Joshi, "Convective heat transfer in curved ducts for a natural circulation system", Journal of Energy, Heat and Mass Transfer, Vol. 18, pp. 39–46, 1987.

[7] J. Eustice, "Flow of water in curved pipes", Proceedings of Royal Society of London, Series A, Vol. 84, pp. 107-18, 1910.

[8] D.Q. Kern, "Process Heat Transfer", McGraw hill, New York, 1986.

[9] J. San, C. Hsu, S. Chen, "Heat transfer characteristics of a helical heat exchanger", Applied Thermal Engineering, Vol. 39, pp. 114-120, 2012.

[10] J. Seara, C. Pontevedra, J.A. Dopazo, "The performance of a vertical helical coil heat exchanger: Numerical model and experimental validation", Applied Thermal Engineering, Vol. 62(2), pp. 680-689, 2014.

[11] J. B. Lee, H.A Simon, J.C.F. Chow, "Buoyancy in developed laminar curved tube flows", International Journal of Heat and Mass Transfer, Vol. 28(2), pp. 631-640, 1985.

[12] N. Padmanabhan, "Entry flow in heated curved pipes", International Journal of Heat and Mass Transfer, Vol. 30(7), pp. 1453-1463, 1987.

[13] A. Gomaa, W.I.A. Aly, M. Omara, M. Abdelmagied, "Correlations for heat transfer coefficient and pressure drop in the annulus of concentric helical coils", Heat Mass Transfer, Vol. 50, pp. 583–586, 2014.

[14] M.M. Mandal, K.D.P. Nigam, "Experimental study on pressure drop and heat transfer of turbulent flow in tube in tube helical heat exchanger", Industrial and Engineering Chemistry Research, Vol. 48(20), pp. 9318–9324, 2009.

[15] M.R. Salem, K.M. Elshazly, R.Y. Sakr R.K. Ali, "Experimental investigation of coil curvature effect on heat transfer and pressure drop characteristics of shell and coil heat exchanger", Journal of Thermal Science and Engineering Application, Vol. 7 / 011005-1, March 2015.

[16] M.R. Salem, K.M. Elshazly, R.Y. Sakr, R.K. Ali, "Effect of coil torsion on heat transfer and pressure drop characteristics of shell and coil heat exchanger", Journal of Thermal Science and Engineering Applications, Vol. 8 / 011015-1, March 2016.

[17] M.R. Salem, K.M. Elshazly, R.Y. Sakr, R. Khalil, "Experimental study on convective heat transfer and pressure drop of water-based nanofluid inside shell and coil heat exchanger", PhD Dissertation, Faculty of Engineering, Benha University, 2014.

[18] R. Remsburg, "Thermal design of electronic equipment", Electronics Handbook Series, Boca Raton: CRC PRESS LLC, 2001.

[19] Y. Mori, S. Nakayama, "Study on forced convective heat transfer in curved pipes (3rd report, theoretical analysis under the condition of uniform wall temperature and practical formulae)", International Journal of Heat and Mass Transfer, Vol. 10, pp. 681-695, 1967.

[20] C.M. White, "Friction factor and its relation to heat transfer", Transactions of the Institution of Chemical Engineers, vol. 18, pp. 66–86, 1932.

[21] M.R. Salem, M.B. Eltoukhey, R.K. Ali, K.M. Elshazly, "Experimental investigation on the hydrothermal performance of a double-pipe heat exchanger using helical tape insert", International Journal of Thermal Sciences, Vol. 124, pp. 496-507, 2018.

Nomenclature

A	Area, m^2
Cp	Specific heat, J/kg.°C
d	Diameter, m
h	Convection heat transfer coefficient, $W/m^2.°C$
k	Thermal conductivity, $W/m.℃$
L	Length, m
m	Mass, kg
$\dot{m}$	Mass flow rate, kg/s

Greek Letters

Δ	Differential
δ	Coil curvature ratio
θ	Coil taper angle, °
λ	Coil torsion
μ	Dynamic viscosity, kg/m.s
ρ	Density, kg/m^3

Scripts

N	Number of coil turns	an	Annulus
p	Pitch, m	ave	Average
Q	Heat transfer rate, W	c	Cross sectional
T	Temperature, ^oC or K	i	Inner or inlet or internal
U	Overall heat transfer, $W/m^2.^oC$	LM	Logarithmic mean
u	Axial velocity, m/s	m	Mean
$\dot{V}$	Volume flow rate, m^3/s	o	Out or outer
Dimensionless Groups		s	Surface
$\overline{Nu}$	Average Nusselt number	t	Tube
De	Dean Number		
Pr	Prandtl number		
Re	Reynolds number		
St	Stanton number		